Astronomy & Astrophysics

Probing the evolution of molecular cloud structure[*]

From quiescence to birth

J. Kainulainen[1], H. Beuther[1], T. Henning[1], and R. Plume[2]

[1] Max-Planck-Institute for Astronomy, Königstuhl 17, 69117 Heidelberg, Germany
e-mail: [jtkainul;beuther;henning]@mpia-hd.mpg.de
[2] Department of Physics and Astronomy, University of Calgary, 2500 University Drive NW, Calgary, Alberta T2N 1N4, Canada
e-mail: plume@ras.ucalgary.ca

ABSTRACT

Context. Probability distribution of densities is a fundamental measure of molecular cloud structure, containing information on how the material arranges itself in molecular clouds.
Aims. We derive the probability density functions (PDFs) of column density for a complete sample of prominent molecular cloud complexes closer than $d \lesssim 200$ pc. For comparison, additional complexes at $d \approx 250-700$ pc are included in the study.
Methods. We derive near-infrared dust extinction maps for 23 molecular cloud complexes, using the nicest colour excess mapping technique and data from the 2MASS archive. The extinction maps are then used to examine the column density PDFs in the clouds.
Results. The column density PDFs of most molecular clouds are well-fitted by log-normal functions at low column densities (0.5 mag $< A_V \lesssim 3-5$ mag, or $-0.5 < \ln A_V/\overline{A}_V \lesssim 1$). But at higher column densities prominent power-law-like wings are common. In particular, we identify a trend among the PDFs: active star-forming clouds always have prominent non-log-normal wings. In contrast, clouds without active star formation resemble log-normals over the whole observed column density range or show only low excess of higher column densities. This trend is also reflected in the cumulative forms of the PDFs, showing that the fraction of high column density material is significantly larger in star-forming clouds. These observations agree with an evolutionary trend where turbulent motions are the main cloud-shaping mechanism for quiescent clouds, but the density enhancements induced by them quickly become dominated by gravity (and other mechanisms), which is in turn strongly reflected by the shape of the column density PDFs. The dominant role of the turbulence is restricted to the very early stages of molecular cloud evolution, comparable to the onset of active star formation in the clouds.

Key words. ISM: clouds – ISM: structure – stars: formation – dust, extinction – evolution

1. Introduction

Star formation takes place exclusively in molecular clouds, or more precisely, in the most extreme density enhancements of those clouds. In the current view, the structure of molecular clouds and thereby the occurrence of the density enhancements is heavily affected by the motions induced by supersonic turbulence (e.g. Scalo et al. 1998). The cloud structure is likewise also crucially affected by the self-gravity of gas and magnetic fields inside the clouds. The relative strengths of these cloud-shaping mechanisms are currently under lively debate and regarded as one of the critical open questions in the physics of the interstellar medium (for reviews, see Mac Low & Klessen 2004; McKee & Ostriker 2007).

The impact of supersonic turbulence on the molecular cloud structure is manifested in the structural characteristics of molecular clouds that seem to agree with theoretical predictions and numerical simulations of such turbulence (see e.g. Sect. 2.1 in McKee & Ostriker 2007). One particularly important statistical property is the probability distribution of densities, which describes the probability of a volume dV to have a density between $[\rho, \rho + d\rho]$. This distribution is expected to take a log-normal shape in isothermal, turbulent media not significantly affected

by the self-gravity of gas (e.g. Vázquez-Semadeni 1994; Padoan et al. 1997; Ostriker et al. 1999; Federrath et al. 2008b). The function is pivotal in current theories of star formation: it is used to explain among others the initial mass function of stars, and the star formation rates and efficiencies of molecular clouds (e.g. Padoan & Nordlund 2002; Elmegreen 2008).

The log-normality of the probability distributions of density is reflected also in *column* densities computed from simulations (e.g. Ostriker et al. 2001; Vázquez-Semadeni & García 2001; Federrath et al. 2009). Unfortunately, measuring column densities in molecular clouds is a challenge in astrophysics by itself. The commonly used methods for deriving column densities, i.e. measurements of CO line emission, thermal dust emission, and dust extinction, suffer from various model-dependent effects, and often probe only narrow ranges of physical conditions (e.g. Goodman et al. 2009; Vasyunina et al. 2009).

For the most nearby molecular clouds, dust extinction measurements in the near-infrared provide sensitivity over a relatively wide dynamical range, starting from $N(H_2 + H) \gtrsim 0.5 \times 10^{21}$ cm^{-2} (Lombardi et al. 2006). The highest measurable column densities depend on the limiting magnitude of near-infrared data available; using e.g. 2MASS data, column densities of $\sim 25 \times 10^{21}$ cm^{-2} are reached (e.g. Kainulainen et al. 2006; Lombardi et al. 2006). This broad range together with the independency of such data on the dust temperature makes dust

---

extinction mapping a viable method to study the large-scale, lower-density regions of molecular clouds and thereby test the predictions from simulations of supersonic turbulence.

In this Letter, we present the first results of a study where we utilise a novel near-infrared dust extinction mapping method to study the structural parameters in a large sample of nearby molecular clouds. We focus on the column density PDFs in the clouds, while the presentation of the maps and further analysis is left to a forthcoming paper (Kainulainen et al., in prep.). Our cloud sample forms a complete set of prominent cloud complexes within 200 pc that have an extent of more than ∼4 pc, or are roughly more massive than ∼10^3 $M_\odot$. For comparison, the sample includes some additional clouds up to $d \approx 700$ pc. The method we adopt allows us to determine the column densities over a range that extends to significantly higher column densities than can be probed by CO line emission (due to the freeze-out of molecules), enabling us to study the structural parameters in a regime not widely accessed before.

2. Extinction mapping method

We employed the near-infrared dust extinction mapping technique nicest (Lombardi 2009) to derive extinction maps of nearby molecular clouds. The method was used in conjunction with JHK_S band photometric data from 2MASS (Skrutskie et al. 2006). In nicest, the near-infrared colours of stars, shining through molecular clouds, are compared to the colours of stars in a nearby reference field that is free from extinction and in which the brightness distribution of stars is similar to the on-cloud region. This comparison yields estimates of a near-infrared extinction towards the stars in the molecular cloud region. The extinction values are then used to compute a spatially smoothed map of extinction through the cloud. In the following, we introduce our practical implementation of the method. For the further description of the method itself, we refer to Lombardi & Alves (2001) and Lombardi (2009) (see also Lombardi 2005).

We applied nicest to several fields covering previously known molecular cloud complexes. The clouds included in the study are listed in Table 1. As an example, Fig. 1 shows the extinction map of the Taurus complex. In order to directly compare the maps of different clouds, their physical resolution was selected to be 0.1 pc (2′ at 170 pc distance). This selection corresponds to the Jeans length for a core at $T = 15$ K and $\overline{n} = 5 \times 10^4$ cm^{-3}. The distances adopted for the clouds are listed in Table 1. For the most clouds farther away than 200 pc, we used a physical resolution of 0.6 pc. The PDFs of these clouds are not directly comparable to those whose resolution is 0.1 pc.

Stars that are either embedded inside the cloud or on the foreground with respect to it can bias the derived extinction. To minimise the contribution of such sources, we used catalogues of previously identified cloud members from the literature to directly remove sources. In addition, we used the "sigmaclipping" iteration, i.e. each source towards which the estimated extinction differed by more than 5-sigma from the local average was removed from the sample. Another possible source of bias in the data is that the background stellar density varies among the clouds according to their galactic coordinates. We investigated the possible effect of this on the PDFs by degrading the background stellar density of some clouds that are close to the galactic plane and recomputing the extinction maps. As these experiments had no impact on the results shown in Sect. 3, we did not include any correction for the differences.

The noise in the extinction maps depends on the galactic coordinates and on extinction. Typically, the 3σ-error at low

Table 1. Molecular cloud properties and the derived parameters.

Cloud	D^a	$M_{H2} \times 10^4$	$\overline{A}_V$	σ_{data}	σ_{fit}	$N_{YSO}{}^b$
Star-forming clouds, physical resolution 0.1 pc						
Ophiuchus	119[1]	0.6	2	4.3	0.48[c]	300
Taurus	140[2]	0.81	1.8	1.5	0.49	300
Serpens	259[3]	3.6	3	2.4	0.51	300
Cha I	165[4]	0.23	1.3	1.3	0.35	200
Cha II	150[4]	0.15	1.3	1.0	0.35	50
Lupus III	155[1]	0.11	1.3	0.9	0.35[c]	50
CrA cloud	129[5]	1.2	0.8	1.0	0.44	tens
Lupus I	155[1]	0.29	1.0	0.7	0.43	tens
LDN1228[d]	200[6]	0.23	1.1	0.7	0.32	tens
Pipe	130[7]	0.95	2.5	1.4	0.29[c]	15
LDN134	100[8]	0.13	1.2	0.6	0.39	a few
LDN204[d]	119[1]	0.43	1.9	0.8	0.41	a few
LDN1333[d]	180[9]	0.57	1.2	0.5	0.38	a few
Non-star-forming clouds, physical resolution 0.1 pc						
LDN1719[d]	120[4]	0.53	0.6	0.7	0.50	
Musca	150[4]	0.07	1.0	0.7	0.45	
Cha III	150[4]	0.18	1.3	0.8	0.46	
Coalsack	150[10]	0.5	2.7	1.4	0.28	
Lupus V	155[1]	0.36	1.4	0.7	0.42	
Star-forming clouds, physical resolution 0.6 pc						
Ori A GMC	450[11]	11	1.4	2.8	0.5	>2000
Per cloud	260[12]	2.0	1.7	1.7	0.49	>100
Ori B GMC	450[11]	9.0	1.2	1.7	0.59	>100
Cepheus A	730[13]	3.5	1.5	1.6	0.47	>100
California	450[14]	11	1.4	0.7	0.51	tens

[a] References: (1) Lombardi et al. (2008b); (2) Torres et al. (2007); (3) Straižys et al. (1996); (4) Knude & Hog (1998); (5) Casey et al. (1998); (6) Kun (1998); (7) Lombardi et al. (2006); (8) Mattila (1979); (9) Obayashi et al. (1998); (10) Corradi et al. (1997); (11) Burrows et al. (1993); (12) Cernis (1993); (13) Crawford et al. (1970); (14) Lada et al. (2009).
[b] An order-of-magnitude estimate of the pre-main-sequence star population in the clouds, based on Reipurth (2008).
[c] No good fit was achieved. A rough estimate is given for reference.
[d] The most prominent Lynds dark nebula in the region.

column densities is 0.5−1.5 mag. The extinction measurements "saturate" at about $A_V = 25$ mag. We note that the fractional area where $A_V \gtrsim 25$ mag is small and we are not likely to significantly miss mass due to an inability to probe higher extinctions.

## 3. The column density PDFs for nearby clouds

Figure 2 shows the mean-normalised PDFs of logarithmic column densities for four clouds of the study. Figures 4−6 show the PDFs for 19 other clouds (online only). In these figures and throughout this Letter, we have divided our sample in active and non-active star-forming clouds based on the presence of confirmed young stellar objects in the clouds.

Qualitatively, most PDFs show a log-normal-like peak, followed by a power-law-like extension at higher column densities. The strength of the extension varies, being dominant for some clouds (e.g. Taurus) and absent for others (e.g. Coalsack). For some clouds, the PDF differs from a log-normal shape also at very low column densities (see Sect. 4). Directed by theoretical predictions, we fitted the peaks of the PDFs using log-normal functions:

$$p(s) \sim \exp\left[-\frac{(\ln A_V/\overline{A}_V - m)^2}{2\sigma^2}\right], \tag{1}$$
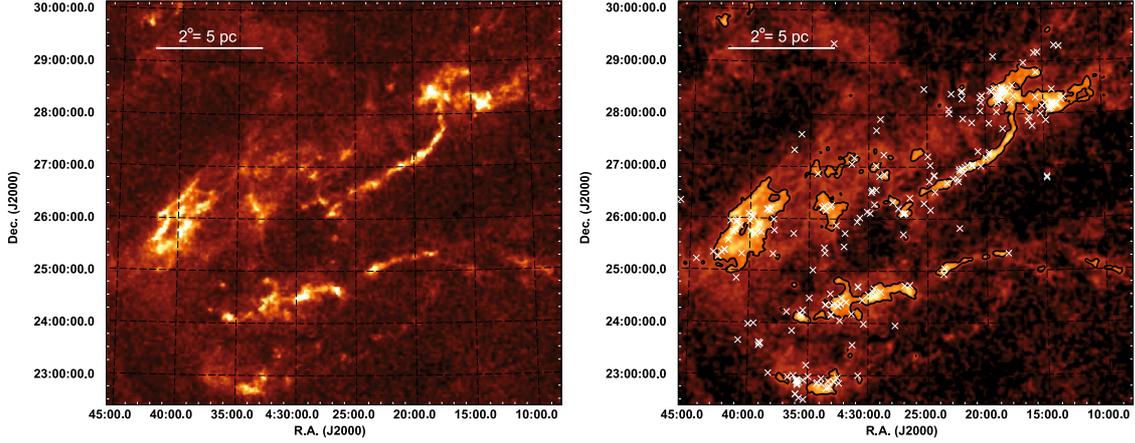
**Fig. 1.** *Left*: wide-field extinction map of the Taurus molecular cloud complex covering ~7.5° × 7.5° (~18 × 18 pc at *d* = 140 pc). The *FWHM* resolution of the map is 2.4′. *Right*: the same, but in logarithmic scaling highlighting the low column density regions. The contour at $A_V = 4$ mag shows the region above which the column density PDF differs from the simple log-normal form. The crosses show the embedded population of the cloud as listed by Rebull et al. (2009).
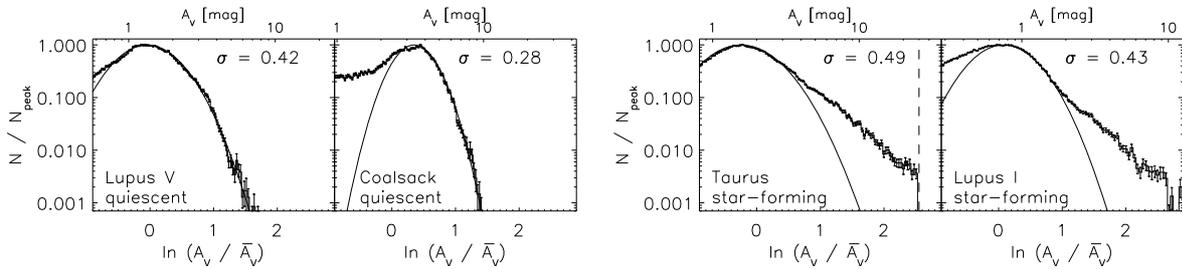
Fig. 2. *Left*: probability density functions (PDFs) of the column density for the non-star-forming clouds Lupus 5 and Coalsack. *Right*: the same for the active star-forming clouds Taurus and Lupus 1. The error bars show the $\sqrt{N}$ uncertainties. Solid lines show the fits of log-normal functions to the distributions around the peak, typically over the range $\ln A_v/\overline{A}_V = [-0.5, 1]$. The dispersions of the fitted functions are shown in the panels. The *x*-axis on top of the panels shows the extinction scale in magnitudes. The vertical dashed line shows the upper limit of extinction values probed by the extinction mapping method. Similar plots for 19 other clouds are shown in Figs. 4−6 (online only).

where $\overline{A}_V$ is the mean extinction, and *m* and σ are the scale and dispersion in logarithmic units. The fits are shown in Figs. 2 and 4−6. Since it is evident that most PDFs are not well fitted by log-normals over their entire range, the fit was typically made over the range $s = [-0.5, 1]$. The dispersions of the fitted log-normal functions are shown in Table 1, and they span the range $\sigma_s \approx 0.3-0.5$. Table 1 also shows the total mass and the mean and standard deviation of the pixels above $A_V = 0$ mag. The total mass was calculated by summing up the extinction values in the map above $A_V = 0.5$ mag and adopting the standard ratio of $N(H_2 + H)/A_V = 9.4 \times 10^{20}$ cm^{-2} (Bohlin et al. 1978).

Another interesting form of the PDFs is the cumulative form of the pixel probability distribution, describing the fractional mass enclosed by an isocontour as a function of column density (or more precisely, the *survival function*). The cumulative PDFs are shown in Fig. 3 for all the clouds of the study. In this figure, the active star-forming clouds are separated from quiescent clouds. Clearly, the fraction of mass in high column density regions is higher in star-forming clouds than in clouds without star formation. We approximated the average cumulative functions for these two classes as a simple mean of all the clouds in the class, which resulted in the relation $(N/N_{peak})_{SF} \approx (N/N_{peak})^{0.4}_{non-SF}$. For example, the star-forming clouds then have roughly one order of magnitude more mass above $A_V = 5$ mag than non-star-forming clouds and more than three orders of magnitude above $A_V = 15$ mag.
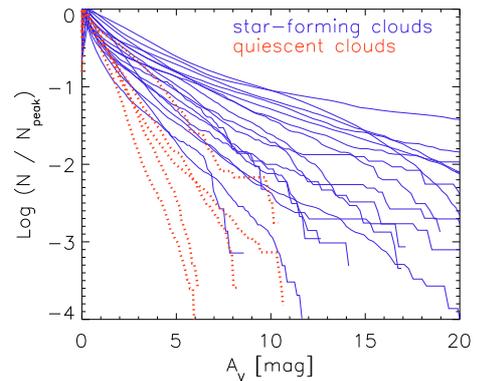
Fig. 3. Cumulative forms of the PDFs shown in Figs. 2 and 4−6. The curves show the fractional mass above the certain extinction threshold (abscissae). Solid blue lines are for clouds that show active star formation and dotted red lines for clouds without active star formation.

4. Discussion and conclusions

While supersonic turbulence is expected to develop a density PDF close to a log-normal distribution, prominent deviations from that shape are predicted in strongly self-gravitating systems (e.g. Klessen 2000; Federrath et al. 2008a). Recent observational studies have indeed indicated that the column density PDFs of molecular clouds are close to log-normal distributions.

For example, Lombardi et al. (2006, 2008a) examined the column density PDFs in the Pipe, Rho Oph, and Lupus molecular clouds. They concluded that the PDF of Ophiuchus is satisfactorily fitted by a log-normal function, while the PDF of Lupus is extremely well fitted by it. However, the PDF of Pipe required four log-normal functions, which they suggested originated from physically distinct components along the line of sight.

The column density PDFs presented in this Letter show that simple log-normal functions fit the PDFs poorly when considering the whole observed column density range, i.e. $N = 0.5-25 \times 10^{21}$ cm^{-2}. As seen in Figs. 2 and 4−6, the PDFs of most clouds deviate from simple log-normality at $s \gtrsim 0.5-1$, or $A_V \gtrsim 2-5$ mag. Even though the log-normals fit the peaks of the PDFs well, the excess "wings" at higher column densities are persistent features of the molecular cloud structure. Likewise, about half of the clouds show non-log-normal features at low column densities. It is, however, difficult to ascertain whether the low column density features are real. It is quite possible that they are mostly residuals caused by other, physically distinct clouds along the line of sight. Nevertheless, they can also be real signatures of cloud structure; non-log-normal features at low column densities have been predicted, related to intermittent fluctuations in turbulent media (e.g. Federrath et al. 2009). We note that the number of pixels in the non-log-normal, higher extinction parts is not small. In fact, the threshold above which the wings become prominent ($A_V \gtrsim 2-5$ mag) is rather low, suggesting that material related to star formation is dominantly located in the non-log-normal part of the PDF. This is illustrated in the right panel of Fig. 1 which shows the extinction map of Taurus with a contour at $A_V = 4$ mag, highlighting the regions belonging to the non-log-normal wing of the PDF. The figure also shows the known pre-main-sequence stars that clearly concentrate on the regions of high column density (Rebull et al. 2009).

Intriguingly, our data appear to show a clear trend. All clouds with active star formation show strong excess of higher column densities (Figs. 2 and 4). In contrast, almost all quiescent clouds have PDFs that either are well described by log-normal functions over the entire column density range, or show relatively low excess of high column densities (Figs. 2 and 5). The trend is obvious for the lower-mass clouds in our sample, but an indication of it is seen also among the more massive clouds (Fig. 6): the active star-forming clouds of Orion have prominent wings compared to the California nebula, a massive cloud with significantly lower star-forming activity (Lada et al. 2009). In the context of turbulent molecular cloud evolution, these observations agree with a picture in which the structure of a molecular cloud in the early stage of its evolution is decisively shaped by turbulent motions. Hence, its column density PDF is close to log-normal, as is the case for the non-active clouds in our sample. As the cloud evolves, prominent local density enhancements can become self-gravitating, which also assembles a growing fraction of the gas to higher column density structures. This significantly alters the simple log-normal form of the column density PDF and is very concretely demonstrated by the cumulative forms of the PDFs (Fig. 3), showing how dramatically the fraction of material at high column density increases from non-active to active clouds. The cumulative PDFs shown in Fig. 3 generalise this trend, suggested earlier by studies of individual cloud complexes (Cambrésy 1999; Lombardi et al. 2006, 2008a; Lada et al. 2009). In the low column density regions of molecular clouds turbulent motions prevail as the dominant structure-shaping mechanism, as indicated by the log-normal-like parts of the PDFs. This appears natural, since those are likely to be the regions where the role of self-gravity remains small.

In this Letter, we have characterised the shape of the column density PDFs in nearby molecular clouds and demonstrated the prevalence of non-log-normalities in them. From the PDFs, we identified a trend that agrees with a picture where self-gravity plays a significant role in shaping the cloud structure starting from a very early stage, corresponding to the formation of first stars in the cloud. An immediate question following these observations is to what extent similar features are present in the simulations of supersonic turbulence. This can be directly addressed by a comparison of our data to simulations that include self-gravity and follow the evolution of cloud structure as a function of time (e.g. Offner et al. 2008; Banerjee et al. 2009). The data presented in this Letter provide a unique set for this purpose, and we are going to address this in a forthcoming paper.

References

Banerjee, R., Vázquez-Semadeni, E., Hennebelle, P., & Klessen, R. S. 2009, MNRAS, 398, 1082
Burrows, D. N., Singh, K. P., Nousek, J. A., et al. 1993, ApJ, 406, 97
Bohlin, R. C., Savage, B. D., & Drake, J. F. 1978, ApJ, 224, 132
Cambrésy, L. 1999, A&A, 345, 965
Casey, B. W., Mathieu, R. D., Vaz, L. P. R., et al. 1998, AJ, 115, 1617
Cernis, K. 1993, Baltic Astron., 2, 214
Corradi, W. J. B., Franco, G. A. P., & Knude, J. 1997, A&A, 326, 1215
Crawford, D. L., & Barnes, J. V. 1970, AJ, 75, 952
Elmegreen, B. G. 2008, ApJ, 672, 1006
Federrath, C., Duval, J., Klessen, R., et al. 2009 [arXiv:0905.1060]
Federrath, C., Glover, S. C. O., Klessen, R. S., & Schmidt, W. 2008a, Phys. Scr. T, 132, 014025
Federrath, C., Klessen, R. S., & Schmidt, W. 2008b, ApJ, 688, L79
Goodman, A. A., Pineda, J. E., & Schnee, S. L. 2009, ApJ, 692, 91
Kainulainen, J., Lehtinen, K., & Harju, J. 2006, A&A, 447, 597
Klessen, R. S. 2000, ApJ, 535, 869
Knude, J., & Hog, E. 1998, A&A, 338, 897
Kun, M. 1998, ApJS, 115, 59
Lada, C. J., Lombardi, M., & Alves, J. F. 2009, ApJ, 703, 52
Lombardi, M. 2009, A&A, 493, 735
Lombardi, M. 2005, A&A, 438, 169
Lombardi, M., & Alves, J. 2001, A&A, 377, 1023
Lombardi, M., Alves, J., & Lada, C. J. 2006, A&A, 454, 781
Lombardi, M., Lada, C. J., & Alves, J. 2008a, A&A, 480, 785
Lombardi, M., Lada, C. J., & Alves, J. 2008b, A&A, 480, 785
Mac Low, M.-M., & Klessen, R. S. 2004, Rev. Mod. Phys., 76, 125
Mattila, K. 1979, A&A, 78, 253
McKee, C. F., & Ostriker, E. C. 2007, ARA&A, 45, 565
Obayashi, A., Kun, M., Sato, F., et al. 1998, AJ, 115, 274
Offner, S. S. R., Klein, R. I., & McKee, C. F. 2008, ApJ, 686, 1174
Ostriker, E. C., Gammie, C. F., & Stone, J. M. 1999, ApJ, 513, 259
Ostriker, E. C., Stone, J. M., & Gammie, C. F. 2001, ApJ, 546, 980
Padoan, P., & Nordlund, Å. 2002, ApJ, 576, 870
Padoan, P., Nordlund, Å., & Jones, B. J. T. 1997, MNRAS, 288, 145
Rebull, L. M., Padgett, D. L., McCabe, C. E., et al. 2009 [arXiv:0911.3176]
Reipurth, B. 2008, Handbook of Star Forming Regions, Volume I-II
Scalo, J., Vazquez-Semadeni, E., Chappell, D., & Passot, T. 1998, ApJ, 504, 835
Skrutskie, M. F., Cutri, R. M., Stiening, R., et al. 2006, AJ, 131, 1163
Straižys, V., Černis, K., & Bartašiūtė, S. 1996, Balt. Astron., 5, 125
Torres, R. M., Loinard, L., Mioduszewski, A. J., & Rodríguez, L. F. 2007, ApJ, 671, 1813
Vasyunina, T., Linz, H., Henning, T., et al. 2009, A&A, 499, 149
Vázquez-Semadeni, E. 1994, ApJ, 423, 681
Vázquez-Semadeni, E., & García, N. 2001, ApJ, 557, 727
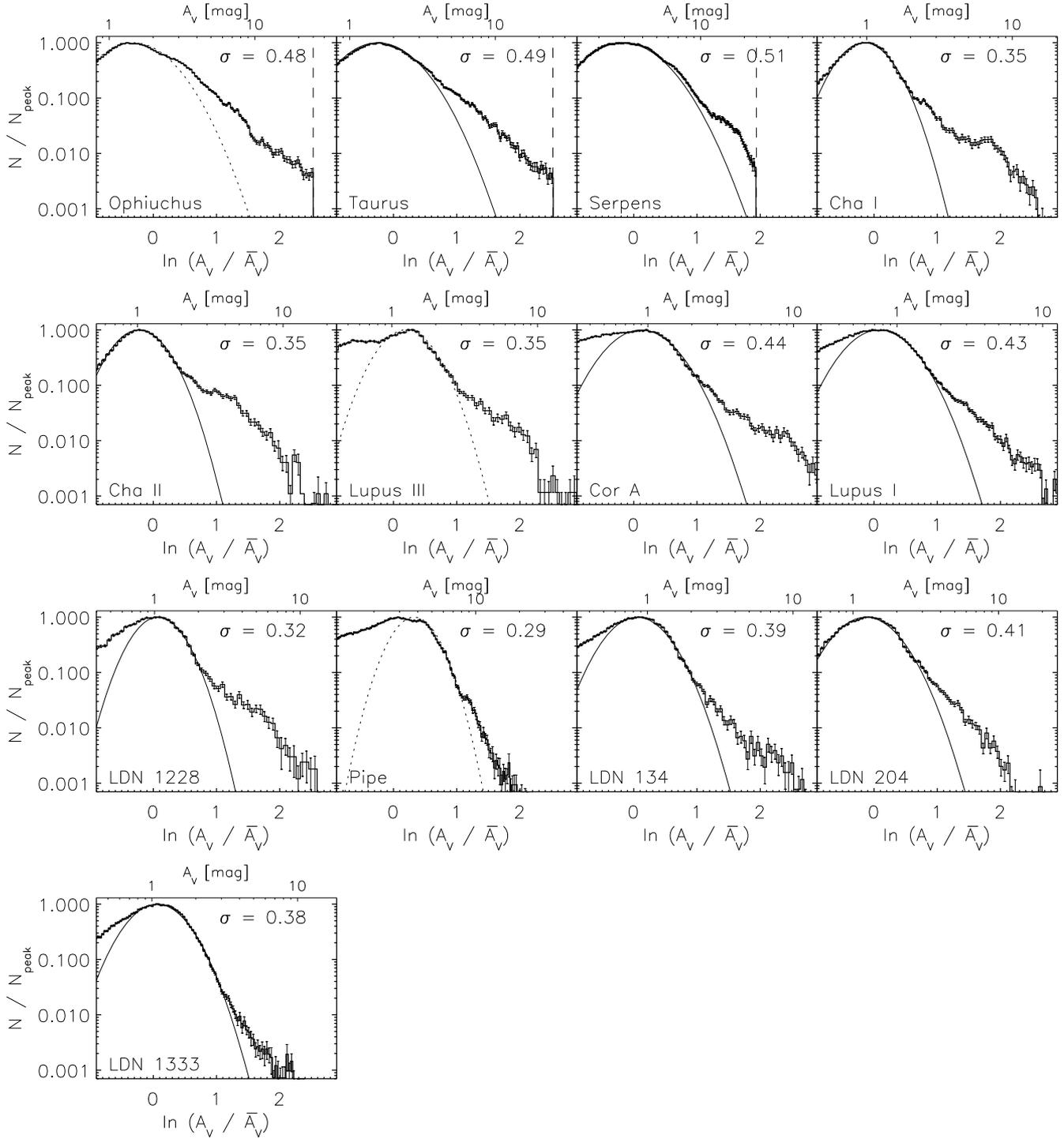
Fig. 4. Probability density functions (PDFs) of a normalised column density for 13 star-forming clouds in the study. The error bars show the $\sqrt{N}$ uncertainties. Solid lines show the fits of lognormal functions to the distributions around the peak, typically over the range $\ln A_v/\overline{A}_V = [-0.5, 1]$. The dispersion of the fitted function is shown in the panels. For some clouds, no reasonable fit was achieved over any A_V range. For those clouds, we show for a reference a function approximating the shape using a dotted line. The x-axis on top of the panels shows the extinction scale in magnitudes.
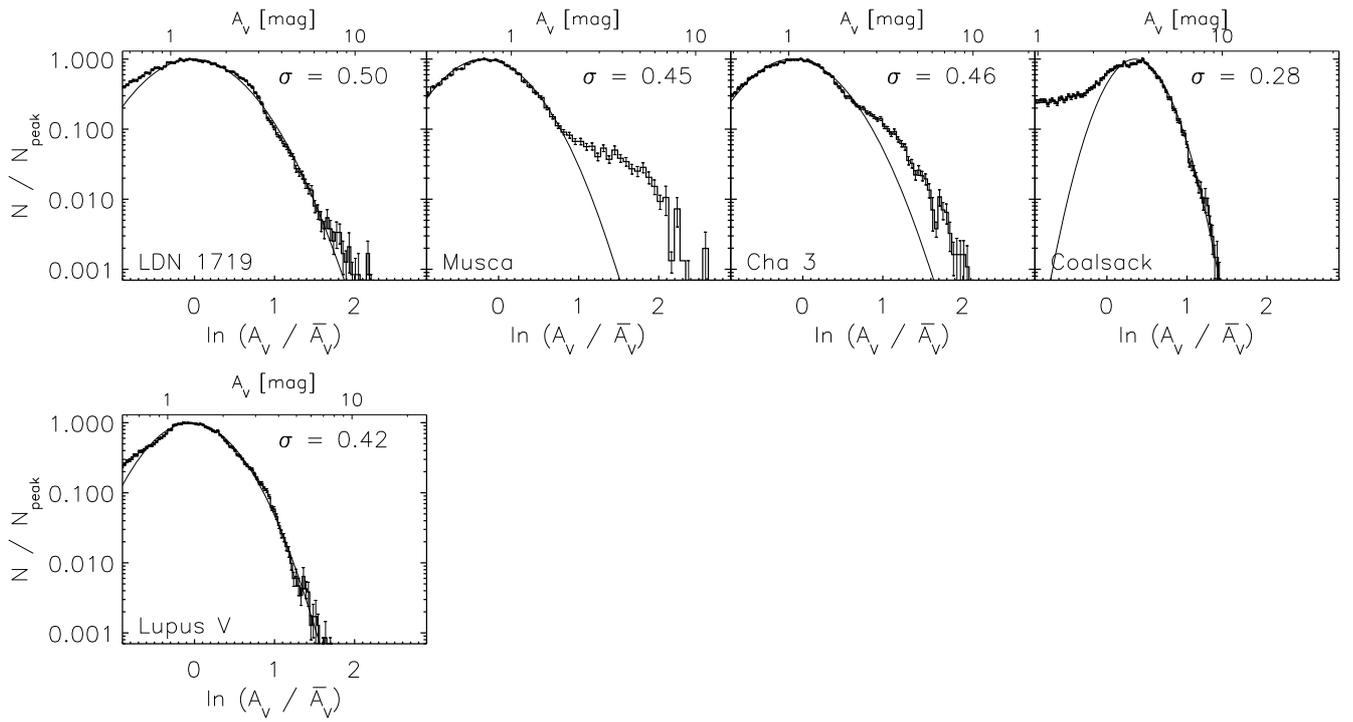
Fig. 5. Same as Fig. 4, but for clouds we classify as clouds not containing active star formation.
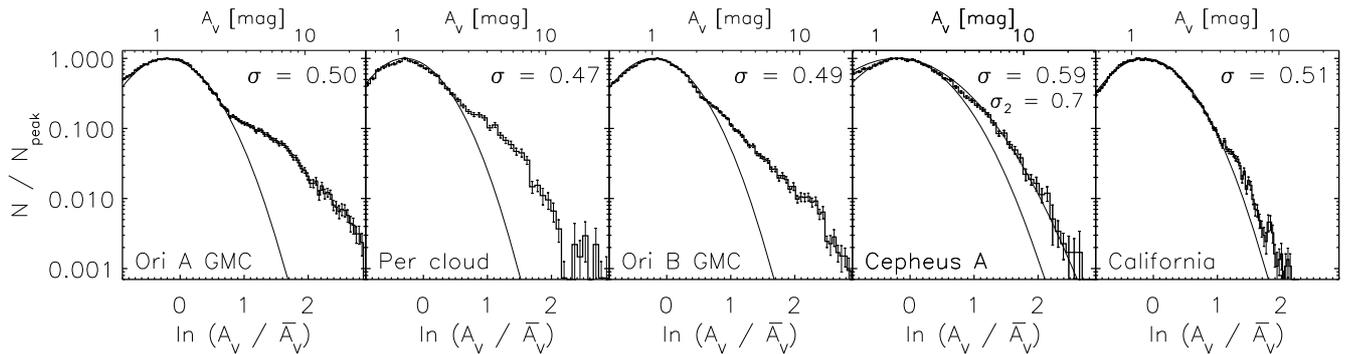
Fig. 6. Same as Fig. 4, but for clouds at varying distances of 250−700 pc. The PDFs are smoothed to the common physical resolution of 0.6 pc. For Cepheus, two equally good fits are shown.